An invasive podosome-like structure promotes fusion pore formation during myoblast fusion

Kristin L. Sens,[1] Shiliang Zhang,[1] Peng Jin,[1] Rui Duan,[1] Guofeng Zhang,[2] Fengbao Luo,[1] Lauren Parachini,[1] and Elizabeth H. Chen[1]

[1]Department of Molecular Biology and Genetics, Johns Hopkins University School of Medicine, Baltimore, MD 21205
[2]Laboratory of Bioengineering and Physical Science, National Institute of Biomedical Imaging and Bioengineering, Bethesda, MD 20892

Recent studies in *Drosophila* have implicated actin cytoskeletal remodeling in myoblast fusion, but the cellular mechanisms underlying this process remain poorly understood. Here we show that actin polymerization occurs in an asymmetric and cell type–specific manner between a muscle founder cell and a fusion-competent myoblast (FCM). In the FCM, a dense F-actin–enriched focus forms at the site of fusion, whereas a thin sheath of F-actin is induced along the apposing founder cell membrane. The FCM-specific actin focus invades the apposing founder cell with multiple finger-like protrusions, leading to the formation of a single-channel macro fusion pore between the two muscle cells. Two actin nucleation–promoting factors of the Arp2/3 complex, WASP and Scar, are required for the formation of the F-actin foci, whereas WASP but not Scar promotes efficient foci invasion. Our studies uncover a novel invasive podosome-like structure (PLS) in a developing tissue and reveal a previously unrecognized function of PLSs in facilitating cell membrane juxtaposition and fusion.

Introduction

Cell–cell fusion is required for the conception, development, and physiology of multicellular organisms (for review see Chen and Olson, 2005; Chen et al., 2007; Oren-Suissa and Podbilewicz, 2007). Among the variety of cell–cell fusion events, fusion between mononucleated myoblasts to form multinucleated myotubes is a critical step during skeletal muscle differentiation, maintenance, and repair. Myoblast fusion in *Drosophila* leads to the formation of larval body wall muscles, which are functionally equivalent to skeletal muscles in vertebrates (for review see Baylies et al., 1998). In *Drosophila*, fusion occurs between two types of muscle cells, muscle founder cells and fusion-competent myoblasts (FCMs; for review see Abmayr et al., 2008; Rochlin et al., 2010). Interactions between these two muscle cell types are mediated by heterotypic cell adhesion molecules, Dumbfounded (Duf)/Kirre and Roughest/IrreC on founder cells (Ruiz-Gómez et al., 2000; Strünkelnberg et al., 2001), and Sticks and stones (Sns) and Hibris on FCMs (Bour et al., 2000; Artero et al., 2001; Dworak et al., 2001; Shelton et al., 2009). In muscle founder cells, the fusion signal is transduced from Duf to the small GTPase Rac via a founder cell–specific adaptor protein Antisocial (Ants)/Rols7 (Chen and Olson, 2001; Menon and Chia, 2001; Rau et al., 2001) and a putative guanine nucleotide exchange factor (GEF) for Rac, Myoblast City (Erickson et al., 1997; Brugnera et al., 2002). In addition, Loner, a GEF for the ARF family of GTPase, is required for the proper localization of Rac (Chen et al., 2003). Rac, in turn, is thought to promote the activation of Scar, a Wiskott-Aldrich syndrome protein (WASP) family member that functions as an actin nucleation-promoting factor (NPF) for the Arp2/3 complex (for review see Stradal and Scita, 2006; Takenawa and Suetsugu, 2007; Kurisu and Takenawa, 2009). In FCMs, Sns signals to WASP via an FCM-specific protein Solitary (Sltr)/dWIP, the *Drosophila* homologue of the WASP-interacting protein (WIP; Kim et al., 2007; Massarwa et al., 2007; Schäfer et al., 2007). In addition, Rac also plays a role in localizing Scar to specific subcellular locations, including sites of fusion, in FCMs (Gildor et al., 2009). These molecular events lead to dramatic rearrangements

K.L. Sens and S. Zhang contributed equally to this paper.

P. Jin and R. Duan contributed equally to this paper.

Correspondence to Elizabeth H. Chen: echen@jhmi.edu

Abbreviations used in this paper: Ants, Antisocial; Duf, Dumbfounded; FCM, fusion-competent myoblast; HPF/FS, high pressure freezing/freeze substitution; MMD, multiple membrane discontinuity; NPF, nucleation-promoting factor; PLS, podosome-like structure; Sltr, Solitary; Sns, Sticks and stones; WASP, Wiskott-Aldrich syndrome protein; WIP, WASP-interacting protein.

The Rockefeller University Press $30.00
J. Cell Biol. Vol. 191 No. 5 1013–1027
www.jcb.org/cgi/doi/10.1083/jcb.201006006

of the actin cytoskeleton, manifested by the formation of a dense, F-actin–enriched structure (known as F-actin focus or plug) at the site of fusion (Kesper et al., 2007; Kim et al., 2007; Richardson et al., 2007). Live imaging showed that these actin foci are transient structures (with an average lifespan of ∼12 min), which form and abruptly dissolve before each fusion event (Richardson et al., 2007; Video 1). Despite a requirement for actin polymerization in myoblast fusion, the cellular localization and function of the actin foci and the role of the Arp2/3 NPFs Scar and WASP in the formation and dissolution of these foci remain unclear.

The WASP family proteins regulate the actin cytoskeleton via activation of the Arp2/3 complex (for review see Stradal and Scita, 2006; Takenawa and Suetsugu, 2007; Kurisu and Takenawa, 2009). Although the mammalian WASP family contains five members (WASP, N-WASP, WAVE1–3), *Drosophila* has one WASP (known as *Wsp*) and one WAVE (known as *Scar*; Ben-Yaacov et al., 2001; Zallen et al., 2002). The mammalian WASP and WAVE have been extensively studied. WAVE is crucial for the formation of lamellipodia, which are broad membrane protrusions (0.1–0.2 µm) filled with branched actin filaments at leading edges of migrating cells (Small et al., 2002). WASP was initially implicated in the formation of filopodia, which are slender cytoplasmic projections filled with bundles of actin filaments (for review see Mattila and Lappalainen, 2008). Recent studies have revealed a central role of WASP in the formation of podosomes and invadopodia, collectively known as invadosomes (for review see Linder, 2009). Podosomes are dynamic actin-dependent adhesive structures observed in many cell types, including monocytic, endothelial, and smooth muscle cells, whereas invadopodia are mostly found in invasive cancer cells (Gimona et al., 2008). Each podosome is composed of a dot-like central F-actin core and a peripheral ring of adhesion molecules (Albiges-Rizo et al., 2009). Although it is commonly assumed that the F-actin cores of podosomes are protrusive, this has not been proven by ultrastructural analysis (Linder, 2009). Both podosomes and invadopodia are associated with ECM degradation, which contributes to cellular invasiveness in physiological and pathological contexts (Linder, 2007). To date, most studies of podosomes and invadopodia have been done in cultured cells, except for an ex vivo study of the endothelium of arterial vessels (Rottiers et al., 2009), as well as ultrastructural studies of leukocyte "invadosome-like protrusions" (ILPs) formed on endothelium (Carman et al., 2007; Carman, 2009) and podosomes in smooth muscle cells of an microRNA knockout model (Quintavalle et al., 2010). It remains to be demonstrated whether podosomes exist in developing tissues of intact organisms and if so, how they behave in a three-dimensional tissue environment.

In this study, we characterize the cellular mechanisms underlying myoblast fusion, focusing on the F-actin–enriched structures at sites of fusion. We show that the F-actin focus is exclusively localized in the FCM, whereas a thin sheath of F-actin is induced along the apposing founder cell membrane. Moreover, the FCM-specific actin focus is a podosome-like structure that invades the apposing founder cell and creates an inward curvature on the founder cell plasma membrane. Using electron microscopy, we show that the invasive actin focus projects multiple finger-like protrusions, which evolve into a single-channel fusion pore between two fusing cells. We further demonstrate that WASP and Scar are the major NPFs required to induce the formation of the asymmetric F-actin–enriched structures at the site of fusion, and loss of WASP or Sltr impairs the invasive behavior of FCMs and causes inefficient fusion pore formation. Thus, we have identified a podosome-like structure that promotes membrane juxtaposition and fusion pore formation in an intact developing tissue.

Results

The F-actin–enriched structure at the site of fusion is asymmetric and cell type specific

To understand the regulation of actin polymerization at the cellular level, we set out to determine the localization of the dense actin focus relative to the apposing muscle founder cell and FCM. Although our previous studies have revealed that the distribution of F-actin within the focus is biased to the FCM (Kim et al., 2007), double labeling for F-actin and founder cell– or FCM-specific proteins did not allow an unambiguous determination of the sidedness of the actin focus (Fig. S1). We therefore expressed a GFP-actin fusion protein in each muscle cell population and visualized the localization of GFP enrichment (labeled by anti-GFP) relative to the F-actin foci (labeled by phalloidin; Fig. 1, A–F). Expressing GFP-actin in all muscle cells with the *twi-GAL4* driver did not affect myoblast fusion and 100% of F-actin foci were double positive for GFP and phalloidin, demonstrating that GFP-actin was integrated into polymerized F-actin at sites of fusion (Fig. 1, A and B). Expressing GFP-actin in FCMs with the *sns-GAL4* driver also led to GFP-positive foci that coincided with F-actin foci (Fig. 1, C and D). In contrast, expressing GFP-actin in founder cells with the *rP298-GAL4* driver led to diffuse GFP signals that did not correspond to the phalloidin-positive F-actin foci (Fig. 1, E and F; Fig. S2). Thus, the dense F-actin foci reside entirely in FCMs, not founder cells.

FCM-specific localization of the F-actin foci was further confirmed by live imaging. Live embryos expressing *GFP-actin* in all muscle cells (Video 2) or in FCMs (Video 3) exhibited transient GFP-positive foci that appeared and dissolved accompanying muscle growth. However, embryos expressing GFP-actin in founder cells rarely showed GFP-positive foci, despite undergoing a similar period of muscle development (Video 4). Thus, founder cells do not form dense F-actin foci during myoblast fusion and muscle growth. Live imaging further revealed dramatic changes in the foci shape before fusion (Fig. 1 G), which were also observed in fixed samples (Fig. 1, H–K). Thus, using a cell type–specific marking strategy and live imaging, we have unambiguously localized the F-actin foci to FCMs and revealed dynamic shape changes of these foci.

The FCM-specific F-actin focus exhibits an invasive behavior toward the founder cell membrane

Upon close examination of sites of membrane adhesion between founder cells and attached FCMs, we noticed a profound change in membrane curvature associated with the FCM-specific actin foci. In *Drosophila* embryos, founder cells/myotubes reside in

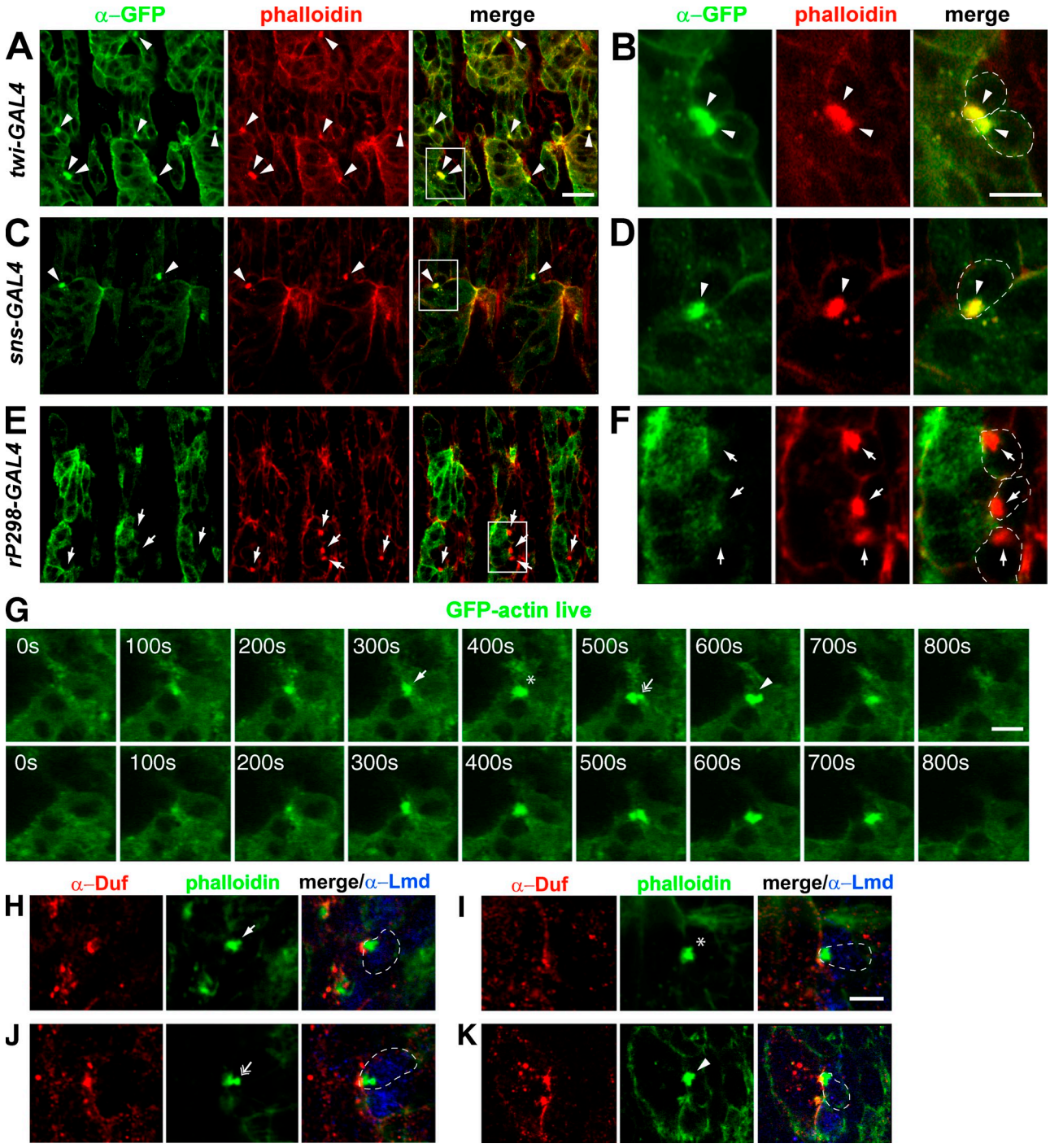

Figure 1. **F-actin–enriched foci specifically localize in FCMs and undergo shape changes during their lifespan.** (A–F) F-actin foci specifically reside in FCMs. Stage 14 wild-type embryos expressing GFP-actin with muscle-specific drivers double labeled with α-GFP (green) and phalloidin (red). Boxed areas in A, C, and E are enlarged in B, D, and F. In this and all subsequent figures, single-slice confocal images are shown and selected muscle cells are outlined (dashed lines) by tracing the cell cortical phalloidin labeling. Note the colocalization of GFP-actin foci with phalloidin-labeled F-actin foci when GFP-actin was expressed in all muscle cells (with *twi-GAL4*; A and B, arrowheads) or in FCMs (with *sns-GAL4*; C and D, arrowheads), and the absence of GFP-actin enrichment at sites of fusion (arrows) when it was expressed in founder cells (with *rP298-GAL4*; E and F). (G) Time-lapse imaging of an F-actin focus in a stage 14 wild-type embryo expressing GFP-actin in all muscle cells (with *twi-GAL4*). Horizontal panels are stills from a time-lapse sequence, and vertical panels are two adjacent optical slices of the same F-actin focus along the Z-axis. (H–K) Four examples of F-actin foci with irregular shapes in fixed wild-type embryos labeled with α-Duf (founder cell; enriched at sites of fusion; red), phalloidin (green), and α-Lmd (FCM; in nuclei; blue; Duan et al., 2001). Note the different foci shapes (indicated by arrow [H], asterisk [I], double-headed arrow [J], and arrowhead [K]) in fixed embryos corresponding to those at different time points (300, 400, 500, and 600 s, respectively) of the live F-actin focus shown in G. Bars: (A, C, and E) 20 µm; (B, D, and F) 10 µm; (G–K) 5 µm.

the top mesodermal layer. Some FCMs reside in the same mesodermal layer as founder cells, although the majority of FCMs reside in deeper cell layers (Beckett and Baylies, 2007). Accordingly, fusion between founder cells/myotubes and FCMs can take place both horizontally (for FCMs residing in the top layer) and perpendicularly (for FCMs residing in deeper layers)

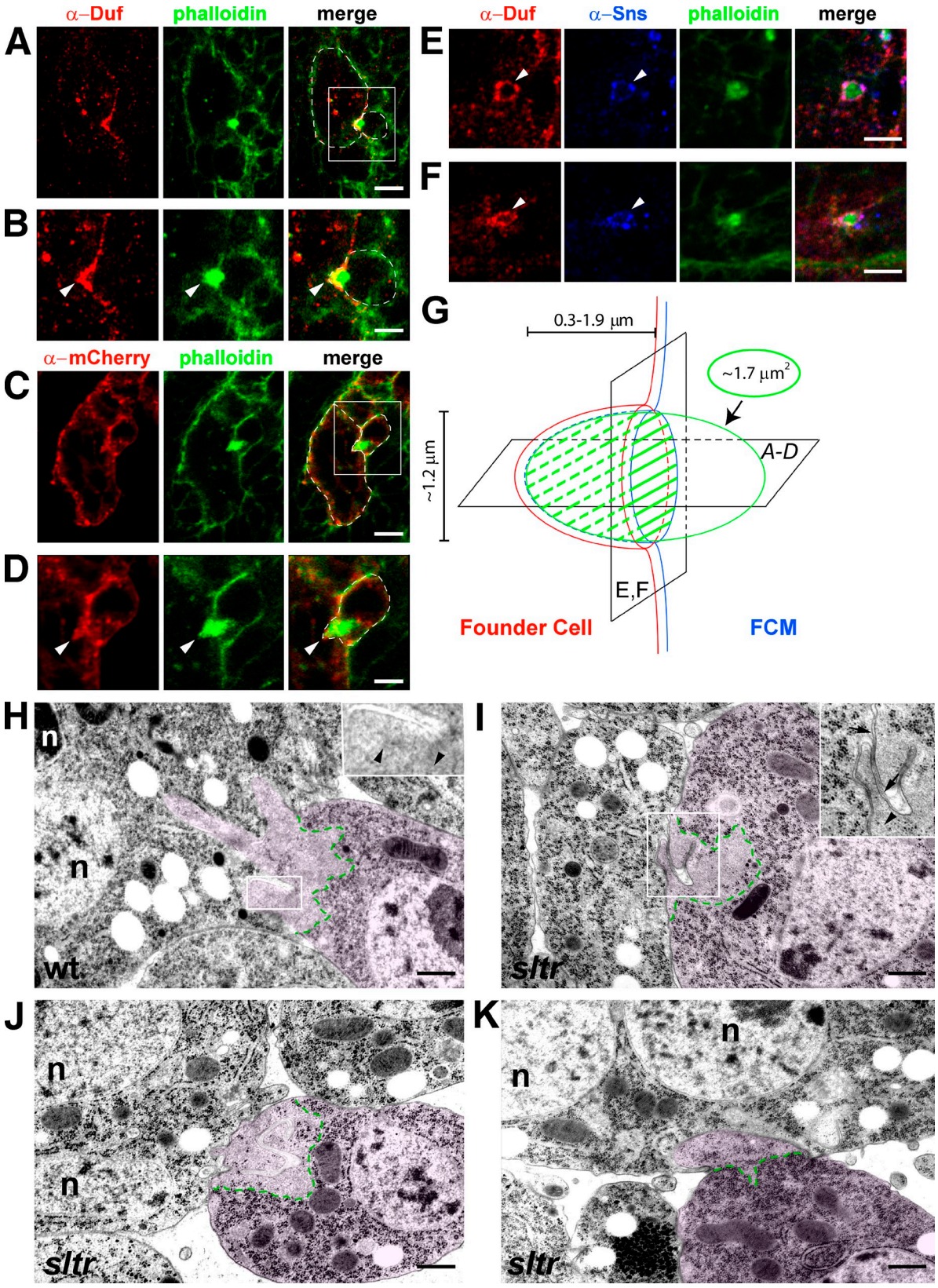

Figure 2. **FCM-specific F-actin foci are invasive and the WASP complex is required for foci invasion.** (A–F) Confocal images of stage 14 wild-type embryos showing horizontal (A–D) and perpendicular (E and F) pairs of founder cell/myotube and FCM. Boxed areas in A and C are magnified in B and D, respectively. Founder cells are outlined in A and C and FCMs in A–D. (A and B) An F-actin focus invading a founder cell. Embryo double labeled with α-Duf (red) and phalloidin (green). Arrowhead indicates the inward curvature on the founder cell membrane. (C and D) Membrane rearrangements at the invasive tip of an F-actin focus. Embryo expressing membrane-targeted mCherry-CAAX in all muscle cells (*with twi-GAL4*) labeled with α-mCherry (red) and phalloidin (green). Arrowhead indicates the invasive tip of the FCM-specific F-actin focus. (E and F) Two examples of F-actin foci encircled by cell adhesion molecules.

relative to the plane of the mesodermal layer. When horizontal pairs of adherent founder cells/myotubes and FCMs were examined, ∼35% (18/52) of the actin foci at a given time point appeared as protrusions that invaded the apposing founder cell and caused an inward curvature, or a "dimple", on the founder cell membrane (Fig. 2, A and B). The average depth of the dimples was 1.0 ± 0.4 µm ($n = 17$) and varied between 0.3 µm (the smallest depth that could be reliably measured) to 1.9 µm, suggesting that the invasion by FCMs is a gradual process. The invasive tips of the FCM-specific F-actin foci colocalized with a membrane-targeted mCherry (mCherry-CAAX), suggesting extensive membrane rearrangements in these areas (Fig. 2, C and D). When we examined perpendicular pairs of adhering founder cells/myotubes and FCMs with horizontal confocal sections, the FCM-specific actin focus was seen encircled by overlapping cell adhesion proteins, Duf and Sns (Fig. 2, E and F). This particular configuration was also observed by Kesper et al. (2007), though the authors proposed that symmetric F-actin structures resided in both the adherent founder cell and FCM. Notably, the F-actin focus within the adhesive rings exhibited nonuniform staining by phalloidin, suggesting the presence of subdomains within a single focus (Fig. 2, E and F). 3D reconstruction of serial confocal sections showed that the invasive F-actin focus resides in a cup-shaped dimple, the wall of which is enriched with Duf and Sns proteins (Video 5 and unpublished data). This unique 3D arrangement of the actin focus and the cell adhesion molecules is consistent with the distinct cellular structures observed in 2D confocal sections and illustrates an asymmetric invasive structure between a founder cell and an FCM (Fig. 2 G).

Ultrastructural analyses reveal FCM-specific, actin-enriched "fingers" invading the founder cell membrane

To examine the asymmetric, FCM-specific invasive structure at a higher resolution, we performed electron microscopy (EM) studies using the high pressure freezing/freeze substitution (HPF/FS) fixation method, which provides better preservation of cellular architecture than the conventional chemical fixation method (McDonald and Auer, 2006). Our HPF/FS EM analyses revealed multiple invasive "fingers" (∼4.3 fingers per FCM, $n = 13$) protruding from the tip of an invading FCM into the apposing founder cell/myotube (Fig. 2 H; Fig. S3, A and B). These invasive structures could also be observed by EM with conventional chemical fixation (Fig. S3 C). These invasive fingers, with a maximum length of 2.0 µm, were enriched with F-actin filaments and devoid of ribosomes and intracellular organelles such as mitochondria (Fig. 2 H; Fig. S3). The average size of the actin-enriched area (1.9 ± 0.8 µm^2, $n = 13$) observed by EM was comparable to that of a single F-actin focus (1.7 ± 0.6 µm^2, $n = 55$) observed under confocal microscopy. The presence of multiple membrane-bound invasive fingers observed by EM correlates with the accumulation of mCherry-CAAX in this area visualized by confocal microscopy (Fig. 2, C and D). Moreover, the varying lengths and directions of the invasive fingers correlate with distinct subdomains and dynamic shape changes of a single F-actin focus revealed by phalloidin labeling (Fig. 1, H–K and Fig. 2, E and F) and live imaging (Fig. 1 G). Taken together, we conclude that the FCM-specific, F-actin–enriched structures visualized by EM and confocal microscopy correspond to the same invasive structure based on their similar sidedness, depth of invasion, size, and morphology.

The WASP and Scar complexes are required for F-actin foci formation

To understand the mechanisms controlling the formation and the invasive behavior of the FCM-specific actin foci, we examined the function of the WASP and Scar complexes. Although both complexes promote Arp2/3-mediated actin polymerization and are required for myoblast fusion, neither complex is indispensable for the formation of F-actin foci, as F-actin foci form and persist through late embryogenesis in the single mutants of the Scar and WASP complexes (Kim et al., 2007; Richardson et al., 2007) (Fig. 3, A–D). To test if these two NPF complexes play redundant functions in F-actin foci formation, we examined double mutant embryos of *scar* and *sltr*. Strikingly, these embryos showed a dramatic reduction of foci size (Fig. 3, E and F) and a near complete block of myoblast fusion (Fig. S4 A, e and f; and Table S1; Berger et al., 2008). Thus, both Scar and WASP complexes are required for F-actin foci formation, and the presence of F-actin foci in single mutants lacking either complex is likely due to function of the other complex. Consistent with this view, loss of *scar* or *kette* resulted in elevated accumulation of Sltr at muscle cell adhesion sites (Fig. 4, compare A with B and C), and conversely, loss of *sltr* led to elevated accumulation of Scar

Embryo triple labeled with α-Duf (red), α-Sns (FCM; enriched at sites of fusion; blue), and phalloidin (green). (G) Schematic drawing of the asymmetric muscle cell adhesion junction. Before fusion, an F-actin focus (green oval) forms at the tip of the FCM (right) and invades the apposing founder cell (left) to create a cup-shaped dimple. The inner wall of the cup is lined with Sns (blue), and the outer wall with Duf (red). Depending on the angle at which the FCM invasion is viewed by confocal microscopy, the cell adhesion molecules can appear as a U-shaped dimple cupping a portion of the actin focus (hatched) in a horizontal section (A–D) or overlapping rings encircling the actin focus in a perpendicular section (E and F). Numbers show average actin foci size (1.7 µm^2), diameter of the adhesive rings (1.2 µm), and depth of invasion (0.3–1.9 µm). (H) Ultrastructural details of an invasive F-actin focus. An FCM (pseudo-colored pink) projects multiple F-actin–enriched invasive fingers into a binucleated myotube in a stage 13 wild-type (wt) embryo fixed by HPF/FS. Serial sections of this invasive structure are shown in Fig. S3 A. The F-actin–enriched areas within the FCMs (boundary marked by dashed green lines) are identified by their light gray coloration and lack of ribosomes and intracellular organelles. Although actin filaments (7-nm diameter) are difficult to be fixed and visualized by HPF/FS (or conventional chemical fixation) EM, magnified inset shows faint actin filaments (arrowheads) within an invasive finger. (I–K) F-actin foci fail to invade properly in *sltr* mutant embryos. F-actin–enriched fingers in FCMs in stage 14 *sltr* embryos either folded upon each other without extending toward the apposing founder cell (I and J; 8/10 actin foci analyzed show this phenotype), or appear wider and shorter than wild type (K; 2/10). Magnified inset in I shows faint actin filaments (arrowhead), as well as a portion of the founder cell membrane (arrows) pulled into the FCM territory by the folded fingers, which may account for the extensive colocalization between founder cell markers (Duf and Ants) and phalloidin staining in *sltr* mutant embryos revealed by confocal microscopy (Fig. 3 D and Fig. S1, B and E; Kim et al., 2007). n: founder cell/myotube nuclei (H–K). Bars: (A and C) 10 µm; (B, D, E, and F) 5 µm; (H–K) 500 nm.

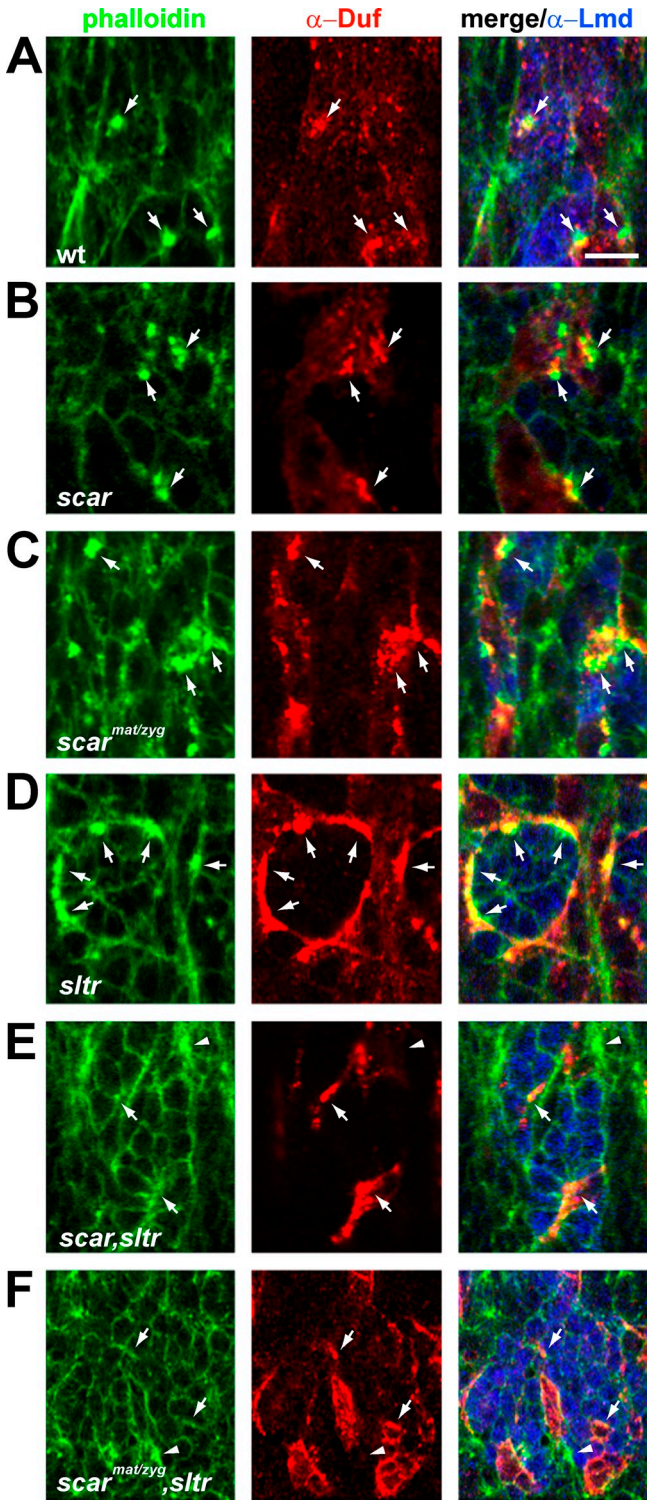

Figure 3. **The WASP and Scar complexes are required for F-actin foci formation at sites of fusion.** Stage 14 wild-type (wt) (A) and stage 15 mutant (B–F) embryos triple labeled with phalloidin (green), α-Duf (red), and α-Lmd (blue). Several muscle cell adhesion sites (marked by Duf enrichment) in each panel are indicated by arrows. In wt embryos, most fusion events occur at stage 14 and there is a decrease in the F-actin foci number in stage 15 (Beckett and Baylies, 2007). Note the persistence of F-actin foci in stage 15 *scar* (B, zygotic null; partial loss of fusion [Fig. S4 A, c]), $scar^{mat/zyg}$ (C, eliminating most, but not all, maternal and zygotic Scar function; near complete loss of fusion [Fig. S4 A, d]), and *sltr* single mutant embryos (D), and the dramatic reduction of F-actin foci in *scar,sltr* (E) and $scar^{mat/zyg}$,*sltr* (F) double-mutant embryos. In *scar,sltr* double mutant embryos, a large percentage (76%; 35/46) of muscle cell adhesion sites are not associated with any F-actin enrichment. The average size for the remainder (11/46) of F-actin foci is 1.2 ± 0.6 μm^2. Arrowheads in E and F indicate actin polymerization in nonmuscle cells (Duf- and Lmd-negative). Bar, 15 μm.

at these sites (Fig. 4, compare D with E). Taken together, we conclude that the Scar and WASP complexes are the major NPFs that play redundant functions in the formation of F-actin foci.

The F-actin foci in mutants lacking the Scar or the WASP complex are FCM specific

The colocalization of Sltr and F-actin foci in *scar* or *kette* mutant embryos (Fig. 4, B and C) suggests that these foci may also be FCM specific. Indeed, in *kette* mutant embryos, expressing GFP-actin in FCMs but not founder cells resulted in colocalization of GFP- and phalloidin-positive foci (Fig. 5, A and B), demonstrating that the enlarged F-actin foci in *kette* mutant embryos reside specifically in FCMs.

Unlike the FCM-specific Sltr, Scar is localized to sites of fusion in both founder cells and FCMs (Richardson et al., 2007) (Fig. 4 D), and is required in both cell types for fusion (Fig. S4 B, a–c, and Table S2). The elevated accumulation of Scar in both cell types in *sltr* mutant embryos (Fig. 4 E) prompted us to ask whether the F-actin foci in these mutant embryos are sided or symmetrically localized. Expressing GFP-actin in FCMs of *sltr* mutant embryos resulted in colocalization of GFP- and phalloidin-positive foci (Fig. 5 C). Thus, despite extensive colocalization between F-actin foci and founder cell–specific markers Duf and Ants observed by confocal microscopy (Kim et al., 2007; Fig. 3 D; Fig. S1, B and E), the F-actin foci in *sltr* mutant embryos specifically reside in FCMs.

The WASP complex promotes efficient invasion of the actin foci

The FCM-specific localization of the F-actin foci in *sltr* and *kette* mutant embryos allowed us to assess whether the WASP or the Scar complex is required for foci invasion into founder cells. Strikingly, the majority of the F-actin foci in *sltr* or *wsp* mutant embryos were not invasive. Only 9% (7/79 foci) in *sltr* mutant embryos and 14% (9/66 foci) in $wsp^{mat/zyg}$ mutant embryos (eliminating both maternal and zygotic WASP) showed any sign of invasion (compared with 35% in wild type). Among these F-actin foci, the depth of invasion was reduced (compare Fig. 5, F and G to Fig. 5 E), with a maximum depth of 0.9 μm in *sltr* and 1.0 μm in $wsp^{mat/zyg}$ mutant embryos (compared with 1.9 μm in wild type). EM studies of *sltr* mutant embryos revealed the ultrastructural details of these abnormal F-actin foci (Fig. 2, I–K). The majority of the foci examined (8/10) exhibited noninvasive F-actin–enriched fingers, which often folded upon each other without extending toward the apposing founder cell (Fig. 2, I and J). Occasionally, invasive actin-enriched fingers appeared to deform the founder cell membrane (2/10 foci; Fig. 2 K). However, these fingers were fewer in number (1–2/per focus compared with 4.3 in wild type) and shorter and wider than normal (Fig. 2, compare H with K), suggesting that their invasiveness was compromised. In contrast to the compromised invasion in

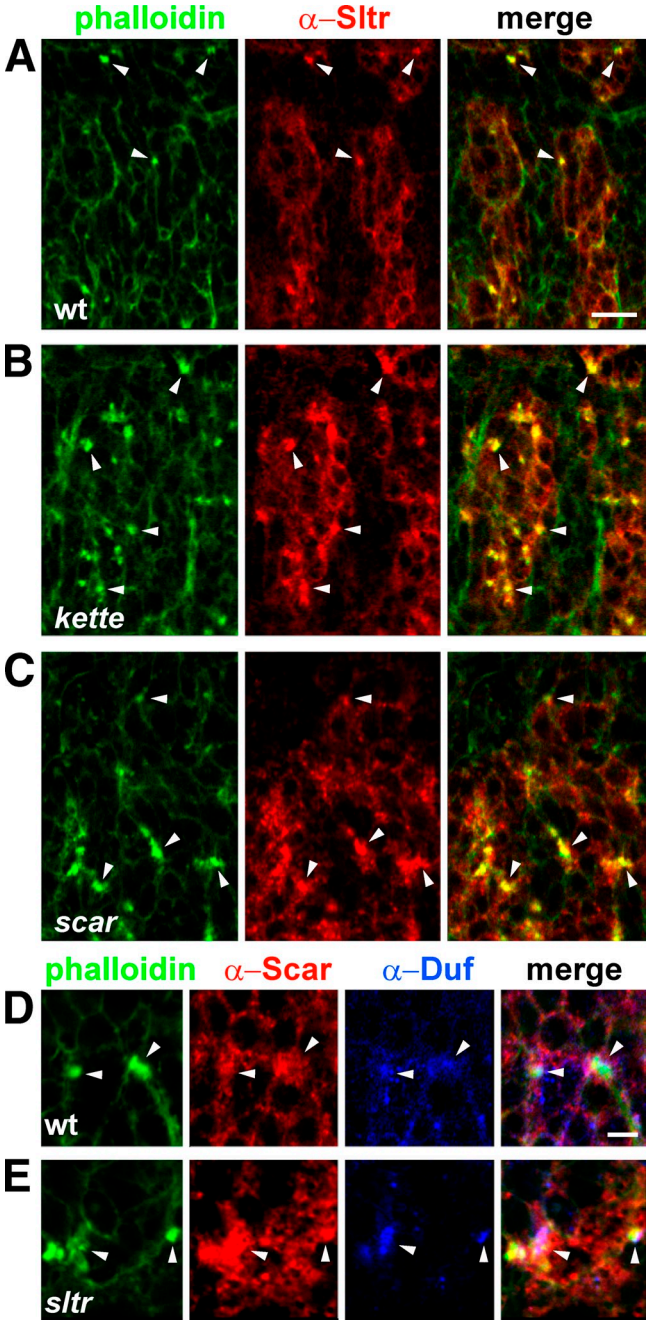

Figure 4. **Increased accumulation of Sltr and Scar at muscle cell adhesion sites in *scar* and *sltr* mutant embryos, respectively.** (A–C) Embryos double labeled with phalloidin (green) and α-Sltr (red). Sltr colocalizes with F-actin foci at muscle cell adhesion sites (arrowheads) in stage 14 wild-type (wt) embryo (A), and with enlarged F-actin foci in stage 15 *kette* (B) and *scar* (C) mutant embryos. (D and E) Embryos triple labeled with phalloidin (green), α-Scar (red), and α-Duf (blue). Scar is localized in both founder cell and FCMs (arrowheads) in a broader domain than the FCM-specific F-actin foci in stage 14 wt embryo (D). In a *sltr* mutant embryo, an elevated level of Scar (arrowheads) is observed at muscle cell adhesion sites. Bars: (A–C) 20 µm; (D and E) 5 µm.

embryos lacking the WASP complex, *scar* or *kette* mutant embryos had a similar percentage of invasive F-actin foci and depth of invasion compared with wild-type embryos (40% [25/63 foci], 2.0 µm [max] and 0.9 ± 0.3 µm, $n = 17$ [average] in *kette*; 42% [30/71 foci], 1.7 µm [max] and 1.0 ± 0.3 µm, $n = 26$ [average] in $scar^{mat/zyg}$; compare Fig. 5, H and I to Fig. 5 E). Thus, the WASP, but not the Scar, complex is required for efficient invasion of the FCM-specific F-actin foci. Consistent with their distinct roles in regulating F-actin foci dynamics, the fusion defect in *sltr* mutant embryos could not be rescued by transgenic expression of Scar (Fig. S4 B, d; and Table S2). Thus, the WASP and Scar complexes in FCMs play redundant roles in F-actin foci formation but distinct functions in actin foci invasion.

The Scar complex is required for the formation of a thin sheath of actin at the site of fusion in the founder cell

After establishing the mechanisms underlying F-actin foci formation and invasion in FCMs, we set out to determine how actin polymerization is regulated in founder cells. Despite the requirement for the Scar complex in founder cells, we did not detect any actin-enriched structures in founder cells when GFP-actin was specifically expressed in this cell population (Fig. 1, E and F). We reasoned that the Scar-mediated actin polymerization in founder cells might be too subtle and/or transient to be reliably detected in wild-type embryos. However, this diminutive and/or transient actin polymerization may become visible in certain fusion-defective mutants, in which founder cells and FCMs have adhered with each other but are prevented from proceeding to subsequent steps of fusion. Indeed, when GFP-actin was specifically expressed in founder cells of late-stage *sltr* embryos we observed actin enrichment that appeared as a thin sheath along the founder cell membrane at muscle cell adhesion sites (Fig. 5 D). In contrast, no actin enrichment was observed in founder cells in late-stage *kette* mutant embryos (Fig. 5 B), suggesting that such actin enrichment requires the Scar complex. Therefore, both the WASP and Scar complexes promote the formation of actin foci in FCMs, but the Scar complex mediates the formation of transient F-actin sheaths in founder cells.

Myoblast fusion is mediated by a single-channel fusion pore

How do the asymmetric actin structures regulate plasma membrane fusion? A hallmark of a membrane fusion event is fusion pore formation. Previous EM analyses in *Drosophila* described fusion pores as multiple membrane discontinuities (MMDs) between two fusing muscle cells (Doberstein et al., 1997). This led to the prevailing view that myoblast fusion is mediated by a series of fusion pores (~50–200 nm in diameter) along the muscle cell contact zone. However, these EM studies used conventional chemical fixation, which is prone to artifacts including membrane discontinuities (Zhang and Chen, 2008; Fig. 6, A–C), even in cell types that do not undergo cell–cell fusion (Fig. 6 D). We therefore reexamined fusion pore morphology using the HPF/FS method. From 510 serial cross sections of HPF/FS fixed stage 14 wild-type embryos (~470 serial sections of 70-nm thickness covers an entire embryonic segment), we observed no cases of MMDs (Fig. 6 E). Instead, each fusion pore that we observed ($n = 10$) appeared as a single-channel opening (ranging from 300 nm to 1.5 µm in diameter; referred to as "macro fusion pores" hereafter) between a pair of muscle cells (Fig. 7, A and B). Smaller fusion pores were not observed so far, likely due to the

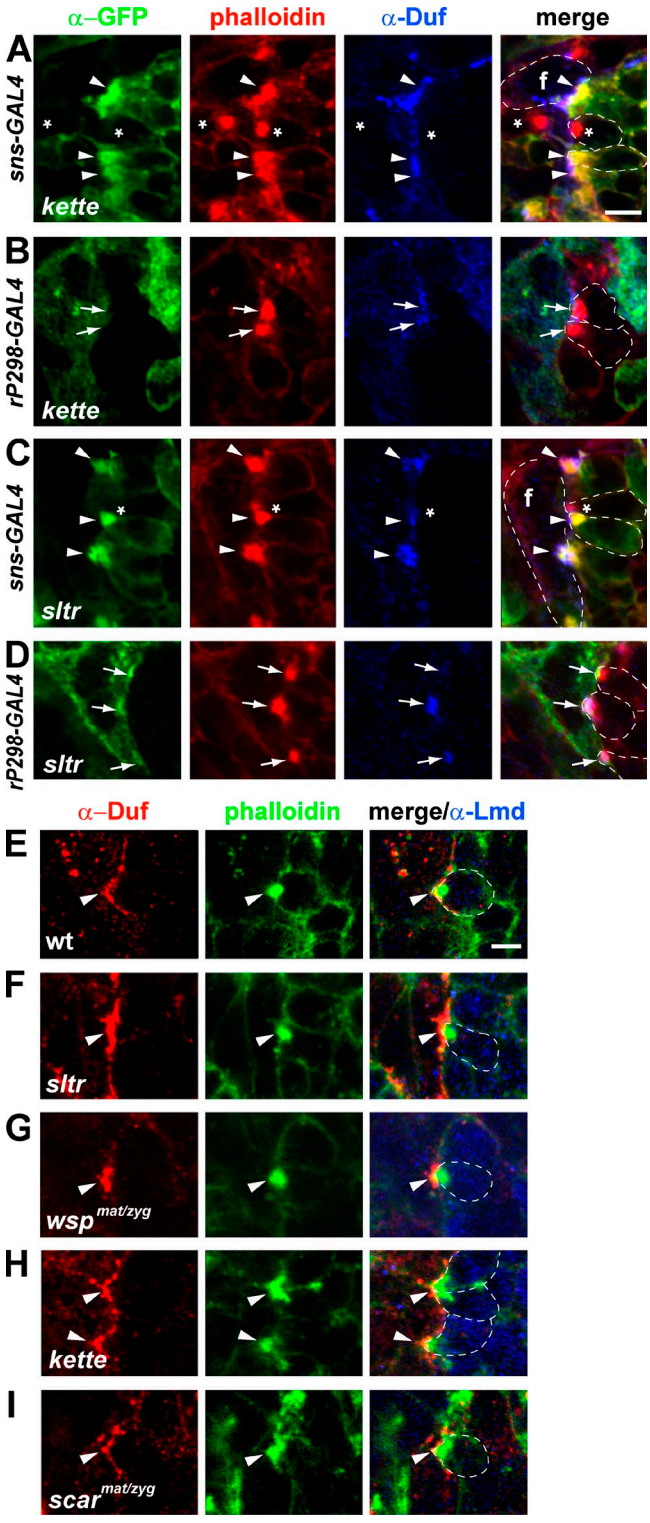

Figure 5. **The FCM-specific F-actin foci in *sltr* and *kette* mutants exhibit different invasive behavior.** (A–D) F-actin foci in *kette* and *sltr* mutant embryos reside in FCMs. Stage 14 (A and C) and stage 15 (B and D) mutant embryos triple labeled with α-GFP (green), phalloidin (red), and α-Duf (blue). *kette* (A and B) or *sltr* (C and D) mutant embryos expressing GFP-actin in FCMs (with *sns-GAL4*; A and C) or in founder cells (with *rP298-GAL4*; B and D) are shown. GFP-negative founder cells (labeled as "f") in A and C are outlined except at sites of cell adhesion with FCMs because the founder cell membranes at these sites cannot be delineated at this resolution. Note the colocalization of GFP- and F-actin–positive foci at muscle cell adhesion sites when GFP-actin was expressed in FCMs (A and C; arrowheads). Also note that in *sltr* (D), but not *kette* (B) mutant embryos, founder cell–expressed GFP-actin showed slight enrichment (arrows) along the cell membrane adjacent to the FCM-specific F-actin foci. Asterisks in A and C mark FCMs that are yet to express GFP-actin. (E–I) F-actin foci in *sltr* and *kette* mutants show different invasive behavior. Stage 14 wild-type (E, wt) and stage 15 *sltr* (F), $wsp^{mat/zyg}$ (G, eliminating both maternal and zygotic WASP), *kette* (H), or $scar^{mat/zyg}$ (I) mutant embryo triple labeled with α-Duf (red), phalloidin (green), and α-Lmd (blue). A typical "invasive" F-actin focus is shown for each genotype. Note the reduced depth of foci invasion (arrowheads) in *sltr* (F) and $wsp^{mat/zyg}$ (G) embryos, and the similar depth of foci invasion (arrowhead) in *kette* (H) and $scar^{mat/zyg}$ (I) embryos, compared with wt (E). Bar, 5 µm.

rapid pore expansion immediately after nascent pore formation, as observed in virus-induced cell fusion (Kaplan et al., 1991; Plonsky and Zimmerberg, 1996; Plonsky et al., 1999). Interestingly, the lumens of the single-channel fusion pores we observed were filled with evenly distributed ribosomes and organelles, indicating active cytoplasmic material exchange between the two fusing cells. This is clearly distinct from the MMDs detected by conventional EM, the "lumens" of which do not contain any cytoplasmic materials (Doberstein et al., 1997; Fig. 6, A–D). Moreover, the single-channel fusion pores were devoid of F-actin or membrane sacs/vesicles (Fig. 7, A and B). Thus, myoblast fusion is mediated by a single-channel macro fusion pore and its expansion is not associated with actin polymerization or membrane vesiculation.

The actin-based invasive structure is required for fusion pore formation

To investigate how the asymmetric F-actin structure at the site of fusion affects fusion pore formation, we performed GFP diffusion assays in mutants of WASP or Scar complexes. We expressed cytoplasmic GFP in founder cells in mutant embryos of two independent alleles of *sltr* (*sltr* and *dWIP*) and monitored the presence or absence of GFP in the attached FCMs, with all muscle cells marked by anti-MHC. GFP did not diffuse from founder cells/myotubes into the attached, mononucleated FCMs (Fig. 7, C–F; Fig. S5 A). Similarly, GFP diffusion did not occur in *kette* mutant embryos (Fig. S5 B; Gildor et al., 2009). These results demonstrate that myoblast fusion is blocked before fusion pore formation in these mutants, and that both the Scar and WASP complexes are required for fusion pore initiation.

To complement the GFP diffusion assays, we performed extensive EM studies of *sltr* mutant embryos in which F-actin foci invasion is compromised (Fig. 2, I–K; Fig. 6 F). In a total of 210 cross sections of HPF/FS fixed stage 14 *sltr* mutant embryos, we never observed MMDs as seen in chemically fixed embryos. In addition, we could not find any single-channel macro fusion pore in these sections, likely due to the limited number of sections we have obtained and greatly reduced fusion events in *sltr* embryos (Table S1; Kim et al., 2007). Moreover, all actin foci observed in *sltr* mutant embryos by EM ($n = 10$) were associated with intact plasma membranes of founder cells/myotubes and the apposing FCMs (Fig. 2, I–K), consistent with the lack of GFP diffusion between these cells (Fig. 7, C–F; Fig. S5 A). We conclude from these results that the WASP complex–mediated invasion of the F-actin foci into the founder cell is normally required for the efficient initiation of fusion pores.

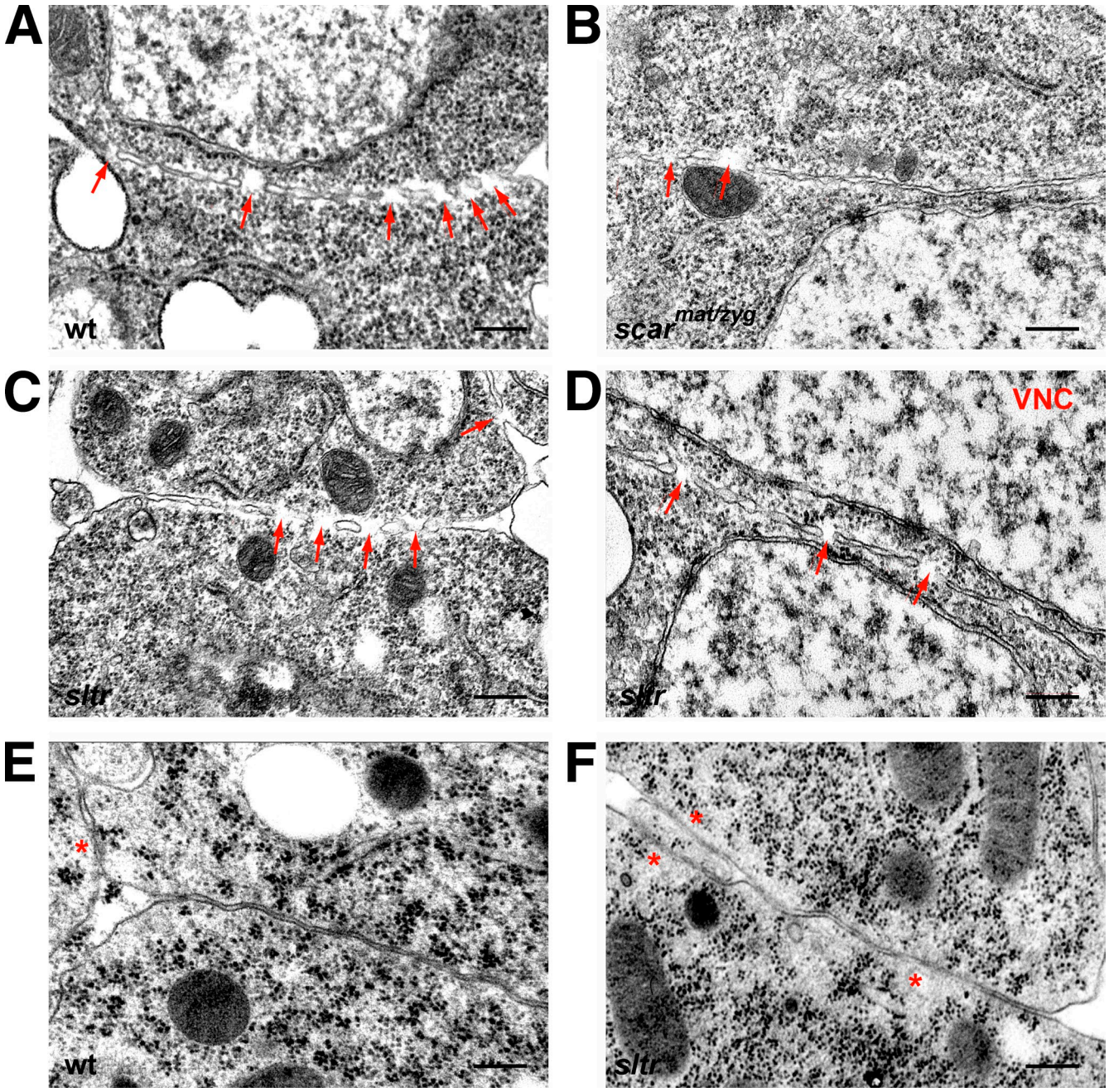

Figure 6. **Myoblast fusion in *Drosophila* is not mediated by a series of fusion pores along the muscle cell contact zone.** Electron micrographs of stage 14 wild-type (A and E, wt), *scar*$^{mat/zyg}$ (B), and *sltr* (C, D, and F) embryos. Samples were prepared by conventional chemical fixation in A–D and by HPF/FS in E and F. (A–D) Multiple membrane discontinuities (MMDs, arrows) are visible along the contact zone of adherent muscle cells in wild-type (A, wt), *scar*$^{mat/zyg}$ (B), and *sltr* (C) embryos. Note that MMDs are also observed between nonfusing cells in the ventral nerve cord (D, VNC). (E and F) Plasma membranes in wt (E) and *sltr* (F) embryos prepared by HPF/FS do not contain discrete MMDs. Asterisks mark "fuzzy" membrane segments that resulted from imperfect fixation. Bar, 200 nm.

Discussion

An invasive podosome-like structure at the tip of an FCM

In contrast to previous models that proposed an even distribution of F-actin on both sides of the apposing membranes of a founder cell and an FCM (Kesper et al., 2007; Richardson et al., 2007), we demonstrate here that the dense F-actin focus resides exclusively in the FCM. Several lines of evidence suggest that this F-actin–containing cell-adhesive structure at the tip of an FCM closely resembles a podosome. First, it comprises an F-actin focus encircled by a ring of adhesive molecules, a configuration that is characteristic of all podosomes (for review see Linder, 2009). Second, it invades and deforms the apposing founder cell membrane by extending multiple finger-like protrusions, consistent with the common assumption that podosomes are protrusive (for review see Carman, 2009; Linder, 2009). Third, the F-actin focus in the FCM and the F-actin core

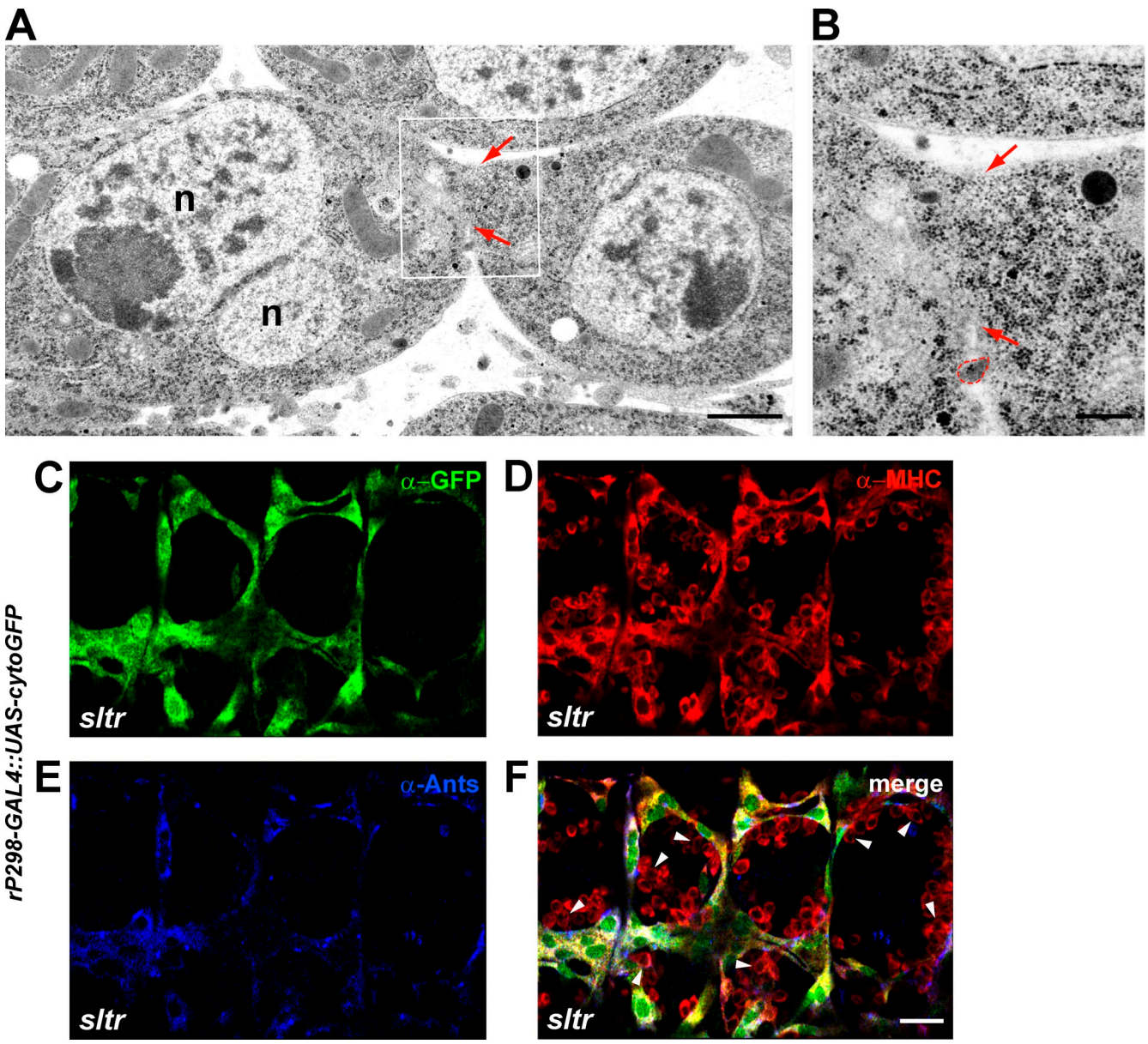

Figure 7. **Myoblast fusion is mediated by a single-channel fusion pore and the WASP–Sltr complex is required for fusion pore formation.** (A and B) A single-channel macro fusion pore revealed by HFP/FS electron microscopy. Boxed area in A is enlarged in B. Arrows indicate boundaries of the fusion pore. Note the even distribution of ribosomes in the lumen of the fusion pore and the absence of F-actin and membrane sacs/vesicles. A small piece of cellular debris between the two cells is outlined in red. n: myotube nuclei. (C–F) Cytoplasmic GFP expressed in founder cells does not diffuse into FCMs in *sltr* mutant embryos. A stage 15 *sltr* mutant embryo expressing GFP in founder cells driven by *rP298-GAL4* triple labeled with α-GFP (green), α-MHC (red), and α-Ants (blue). Mononucleated FCMs do not contain GFP, even though many of them (a few are indicated by arrowheads) have attached to elongated founder cells/myotubes. Bars: (A) 500 nm; (B) 200 nm; (C–F) 20 µm.

of a podosome share similar dense morphology, size (~1.2 µm vs. ~1 µm in diameter), and dynamics (~12 min vs. 2–12 min average lifespan; Richardson et al., 2007; this paper; for review see Albiges-Rizo et al., 2009; Linder, 2009). Lastly, the formation of both structures requires the Arp2/3 NPFs and the Arp2/3 complex (this paper; for review see Albiges-Rizo et al., 2009; Rochlin et al., 2010). Although it remains to be determined if the FCM adhesive structures are associated with ECM degradation activities as described for all in vitro podosomes (for review see Linder, 2007), the many features shared between these two protrusive structures led us to propose the former as a "podosome-like structure" (PLS). It is worth noting that the morphology, size, dynamics, and the invasive nature of the PLSs distinguish them from another type of actin-based cellular protrusion, filopodia (for review see Mattila and Lappalainen, 2008). There are a few notable differences between the PLSs and previously described podosomes. First, the adhesive molecules used by muscle cells are Ig domain–containing transmembrane proteins, instead of integrins and other focal adhesion–related molecules in podosomes (for review see Linder, 2009). Indeed, integrins are not required for *Drosophila* myoblast fusion (Prokop et al., 1998). Second, the F-actin focus in an FCM is surrounded by "double" adhesive rings from both the FCM (Sns ring) and the apposing founder cell (Duf ring), distinct from the

single podosome rings adhering to a 2D matrix. To our knowledge, the FCM-specific adhesive structure represents the first example of an invasive podosome-like structure in an intact developing tissue.

Function of the invasive PLSs in the initiation of fusion pores

Our study implicates the invasive PLSs in the initiation of fusion pores. In *sltr* mutant embryos where PLS invasion is compromised, fusion pores do not form between the majority of founder cell/myotube and FCM pairs. The formation of bi-, tri-, or quadruple-nucleated myotubes in *sltr* mutant embryos is likely due to the inefficient invasion of aberrant F-actin fingers mediated by the Scar complex. We speculate that after the initial muscle cell adhesion mediated by cell adhesion molecules, the invasive fingers of the PLS may apply mechanical/physical forces by pushing against the thin sheath of actin in founder cells, thus bringing the two apposing plasma membranes into even closer proximity. In this regard, invadosome-like protrusions formed during leukocyte invasion of endothelial cells are implicated in bringing apical and basal membranes of endothelial cells together for the formation of transcellular pores (Carman et al., 2007; for review see Carman, 2009). In addition, PLSs may direct ECM protease secretion as shown for in vitro podosomes, which may facilitate closer membrane proximity by degrading adhesion molecules and/or ECM proteins. We note, however, that although invasion of the FCM-specific PLSs into founder cells is required for myoblast fusion, it is not sufficient. Thus, despite the aggressive invasion of the PLSs, mutant embryos lacking the Scar complex are defective in myoblast fusion (Richardson et al., 2007) (Fig. S4 A, c and d). Because the Scar complex is required for the formation of the thin sheath of actin in the founder cells, loss of Scar may render the founder cell membrane less resistant to PLS invasion and thus compromise PLS's ability to bring the two membranes into closer proximity.

Our EM analysis revealed single-channel macro fusion pores between founder cells/myotubes and FCMs, though it is unclear at present whether the multiple invasive fingers of a PLS promote the formation of one or more nascent fusion pores to initiate the fusion process. Interestingly, single-channel macro fusion pores have also been reported in yeast mating and *Caenorhabditis elegans* hypodermal cell fusion (Gammie et al., 1998; Mohler et al., 1998), suggesting that they may represent a common intermediate structure in cell–cell fusion in vivo. Moreover, neither membrane sacs nor vesicle accumulation is associated with the single-channel fusion pores during myoblast fusion, arguing against a role of membrane vesiculation in fusion pore expansion. Consistent with this, membrane vesiculation does not appear to play a role during pore expansion in virus (gp64)-induced fusion of Sf9 cells (Chen et al., 2008).

The Arp2/3 NPFs Scar and WASP promote actin polymerization and fusion pore initiation

Our studies demonstrate that the NPFs for the Arp2/3 complex, Scar (in the heteropentameric Scar complex) and WASP (in complex with Sltr), are the major NPFs for promoting actin polymerization at sites of fusion. This is supported by the recruitment of the two complexes to sites of fusion, the diminished actin polymerization in the *sltr scar* double mutant embryos, and the reciprocal accumulation of each complex in the absence of the other. We note that Gildor et al. (2009) reported enlarged actin foci in *dWIP; twi-GAL4::GFP-Scar* embryos (*twi-GAL4::GFP-scar* caused a *scar* mutant-like phenotype and was considered as a *scar* mutant in that study). However, it is unclear if the green "phalloidin" signal shown by Gildor et al. (2009) was in part contributed by the overexpressed GFP-Scar accumulated at muscle cell adhesion sites. Despite their functional redundancy in F-actin foci formation, the WASP, but not the Scar, complex is required for efficient invasion of the PLSs. We note that the intracellular parasite *Listeria* use a WASP-like protein to generate F-actin–filled comet tails that propel the bacteria to invade neighboring host cells with finger-like membrane protrusions (Tilney and Portnoy, 1989). Thus, the WASP complex can be used in multiple contexts to generate finger-like membrane protrusions.

Our EM studies and GFP diffusion assays demonstrate that fusion pore initiation requires both the Scar and WASP complexes. While a previous report (Gildor et al., 2009) agrees with our finding that the Scar complex is required for fusion pore formation, it was proposed that the WASP–Sltr complex is required for expanding nascent fusion pores, based on the presence of MMDs in *dWIP* and *wsp* mutant embryos by chemical fixation EM, as well as the presence of founder cell–expressed GFP (driven by *rP298-GAL4*) in FCMs in these mutants (Massarwa et al., 2007; Gildor et al., 2009). We find that MMDs are membrane artifacts generated by chemical fixation, and that the commonly used founder cell–specific *rP298-GAL4* drives leaky expression in a small number of FCMs (Fig. S2), which may account for the presence of GFP in FCMs observed in Gildor et al. (2009) and Massarwa et al. (2007). Although the requirement of both Scar and WASP complexes in fusion pore initiation prevented us from examining their role in fusion pore expansion using the respective mutants, the depolymerization of the F-actin foci after pore formation suggests that neither these NPFs nor actin polymerization is likely to be required. In agreement with this, dissociation of the actin cytoskeleton at the fusion site has been shown to be a prerequisite for pore expansion in the virus (gp64)-induced fusion of Sf9 cells (Chen et al., 2008).

Our current studies do not preclude a previously proposed role for the WASP complex in targeted exocytosis of prefusion vesicles, which may be involved in delivering an unknown fusogen, or proteins/chemicals that stimulate fusogen activity, to sites of fusion (Kim et al., 2007). *sltr* mutant embryos prepared by either HPF/FS or chemical fixation showed accumulation of prefusion vesicles that are not associated with the F-actin foci (Kim et al., 2007; unpublished data), consistent with a role for the WASP complex in vesicle targeting (Kim et al., 2007). Thus, the WASP complex may have dual functions in myoblast fusion by promoting PLS invasion and directing vesicle trafficking.

Defining an asymmetric fusogenic synapse

The asymmetric cell adhesive junction characterized in this study and the polarized trafficking of prefusion vesicles to the site of cell adhesion described previously (Doberstein et al., 1997;

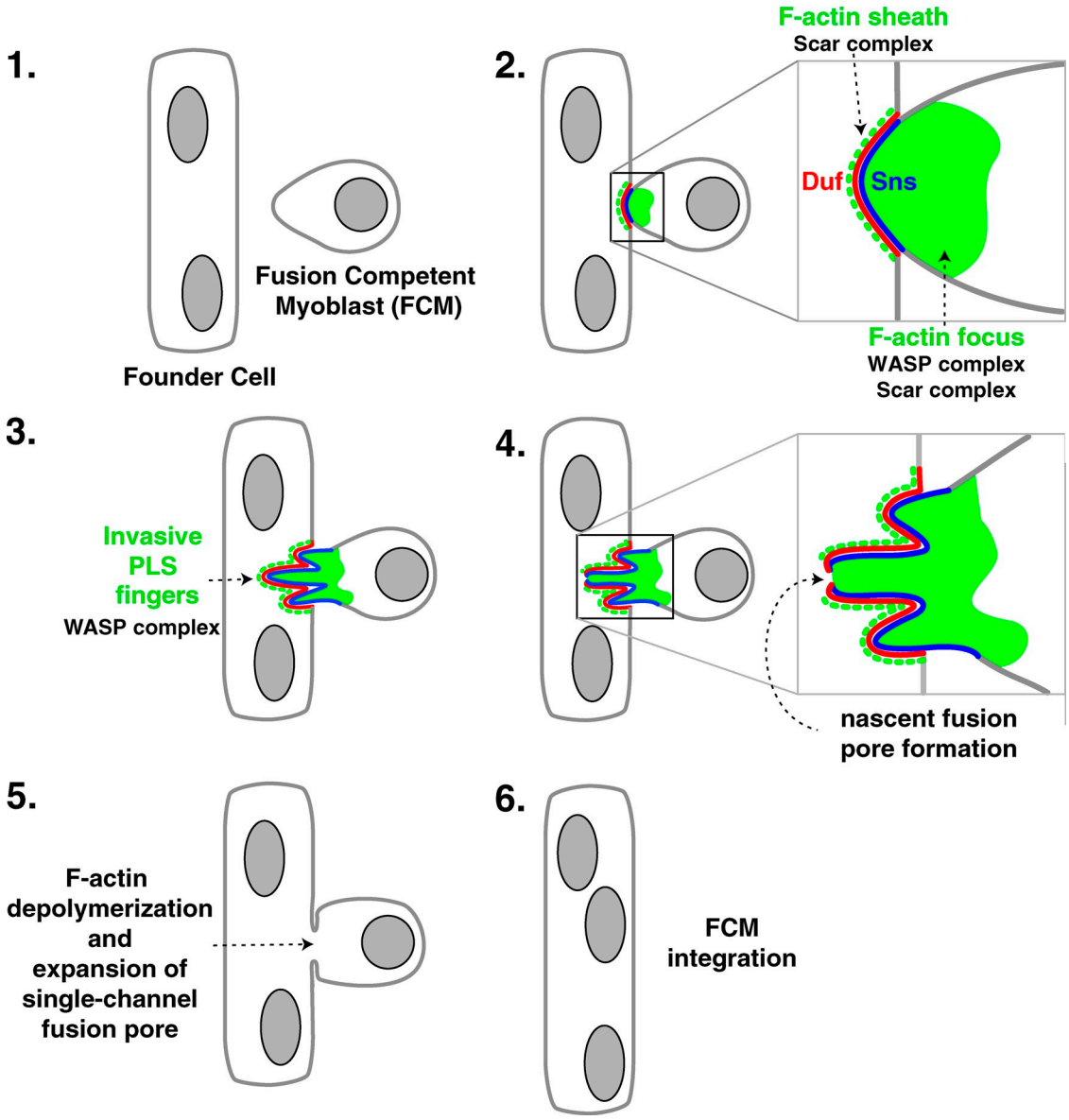

Figure 8. **A model describing the cellular and molecular events at the asymmetric fusogenic synapse.** (1) An FCM is attracted by a founder cell/myotube. (2) The FCM and founder cell/myotube adhere via the interaction of cell adhesion molecules (only Duf and Sns are shown) at the site of fusion. In the FCM, Sns recruits both the Scar and WASP complexes to induce the formation of a dense F-actin focus. In the founder cell, Duf recruits the Scar complex to induce the formation of a thin F-actin sheath. (3) In the FCM, the cell adhesion molecule and the F-actin focus constitute a podosome-like structure (PLS) and, through the action of the WASP–Sltr complex, the PLS protrudes multiple invasive fingers to palpitate the founder cell membrane. (4) We speculate that a nascent fusion pore forms at the tip of a podosome finger, where the two adherent membranes are brought into close proximity through the interactions between the podosome finger in the FCM and the thin sheath of actin in the founder cell. (5) The nascent fusion pore expands to a single-channel macro fusion pore after F-actin depolymerization. (6) The FCM completely incorporates into the founder cell/myotube, contributing one additional nucleus.

Kim et al., 2007) are reminiscent of two types of synapses: the neural synapse and the immunological synapse (Dustin and Colman, 2002; Dillon and Goda, 2005; Salinas and Price, 2005; Billadeau et al., 2007; Stinchcombe and Griffiths, 2007). Although different transmembrane proteins are used for cell adhesion in each context, in all cases the cell adhesion molecules seal an encircled contact zone that serves as a target for polarized transport/secretion of specific vesicles. We therefore suggest that an analogous "fusogenic synapse" exists at the junction between a founder cell and an apposing FCM. The asymmetric fusogenic synapse we have defined in this study differs from the fusion-restricted myogenic-adhesive structure (FuRMAS) proposed by Kesper et al. (2007), which depicted symmetric F-actin accumulation on both sides of the apposing membranes without description of invasive behaviors.

We propose a stepwise model to describe the molecule and cellular events occurring at an asymmetric fusogenic synapse (Fig. 8). First, Duf- and Sns-mediated adhesion between a founder cell and an FCM triggers the recruitment of downstream effectors, including NPFs for the Arp2/3 complex, to the adhesive junction in a cell type–specific manner. Differential activities of the WASP and the Scar complex result in distinct F-actin accumulation on the two sides of the fusogenic synapse. Dynamic interactions between the protrusive PLS fingers in an

FCM and the thin sheath of actin in the apposing founder cell bring the plasma membranes into closer proximity and prime them for fusion. We speculate that this tight membrane juxtaposition facilitates the engagement of an unknown fusogen and/or generates sufficient membrane curvature to initiate the formation of a single-channel fusion pore between the two apposing cells. This is followed by rapid F-actin depolymerization to allow fusion pore expansion and, ultimately, integration of the FCM into the founder cell/myotube. Given that the actin cytoskeleton has been implicated in multiple cell–cell fusion events (Dvoráková et al., 2005; Jay et al., 2007; Pajcini et al., 2008), we suggest that the Arp2/3-mediated, F-actin–based invasive PLSs may be used as a general strategy to facilitate membrane juxtaposition and plasma membrane fusion.

Materials and methods

Fly genetics

Fly stocks were obtained from the Bloomington Stock Center (Bloomington, IN), except for the following: *w*^{1118}, *sltr*^{S1946}*/CyO,actin-lacZ* (Kim et al., 2007); *dWIP* ^{D30} (Massarwa et al., 2007); *kette*$^{J4\text{-}48}$*/TM6B* (Hummel et al., 2000); *scar*^{k13811}*/CyO,actin-lacZ* (Zallen et al., 2002); *scar*$^{\Delta 37}$*/CyO* (Zallen et al., 2002); *FRT*^{82B}, *Wasp*^{3}, *e/TM6B* (Ben-Yaacov et al., 2001); *sns-GAL4* (Kocherlakota et al., 2008); *rP298-GAL4* (Menon and Chia, 2001); *UAS-Scar* and *UAS-mCherry-CAAX* (this paper). A new *scar* mutant allele, *scar*^{S196}, was isolated in a genetic screen for muscle development (see below for details on this allele).

Germline clones of *scar*^{k13811} and *wsp*^{3} were generated as described previously (Ben-Yaacov et al., 2001; Zallen et al., 2002). Double mutant of *scar*^{k13811} and *sltr* ^{S1946} *(scar*$^{mat/zyg}$*,sltr)* was generated by heat shocking *hs-FLP; scar*^{k13811}, *FRT40A, sltr*^{S1946}*/ovoD, FRT40A* larvae and the progeny were crossed with *scar*^{k13811}, *FRT40A, sltr*^{S1946}*/CyO* males. *scar*$^{mat/zyg}$*,sltr* embryos were differentiated from *scar*$^{mat/zyg}$ embryos by the absence of anti-Sltr staining. The *scar*^{S196} allele was used to generate the zygotic double mutant *scar,sltr*.

To express GFP-actin in specific myoblast populations in wild-type embryos, *UAS-Act5C.GFP3* females were crossed with *twi-GAL4*, *sns-GAL4*, or *rP298-GAL4* males, respectively. To express GFP-actin in *sltr* mutant: *sltr*^{S1946}*/CyO, ftz-lacZ; UAS-Act5C.GFP3* females were crossed with either *rP298-GAL4/Y; sltr*^{S1946}*/CyO, actin-lacZ* or *sns-GAL4, sltr*^{S1946}*/CyO, actin-lacZ* males. To express GFP-actin in *kette* mutant: *UAS-Act5C.GFP; kette*$^{J4\text{-}48}$*/TM6B, Ubx-lacZ* females were crossed with either *rP298-GAL4/Y; kette*$^{J4\text{-}48}$*/TM6B, Ubx-lacZ* or *sns-GAL4; kette*$^{J4\text{-}48}$*/TM6B, Ubx-lacZ* males. To express cytoGFP in *sltr* mutant: *sltr, UAS-GFP*^{S65T}*/CyO, actin-lacZ* females were crossed with *rP298-GAL4; sltr/CyO, actin-lacZ* males. In all of these crosses, *sltr* and *kette* mutant embryos were identified by their lack of β-gal expression and their fusion-defective phenotype. To express cytoGFP in *kette*$^{J4\text{-}48}$ and *dWIP* mutants: *UAS-GFP*^{S65T}*/+; kette*$^{J4\text{-}48}$*/+* or *dWIP, UAS-GFP*^{S65T}*/CyO* were crossed with *rP298-GAL4/Y; kette*$^{J4\text{-}48}$*/+* and *rP298-GAL4/Y; dWIP/+* males, respectively. Homozygous *kette*$^{J4\text{-}48}$ and *dWIP* mutants were identified by the loss of fusion phenotype visualized by MHC staining. To express mCherry-CAAX in all muscle cells: *UAS-mCherry-CAAX* males were crossed with *twi-GAL4* females. To examine the mis-expression of the *rP298-GAL4* driver in FCMs: *rP298-GAL4* females were crossed with *UAS-lacZNZ (UAS-lacZ-nls)* males.

Rescue crosses were performed as followed: Scar rescue of scar–scar$^{\Delta 37}$/CyO, arm-GFP; UAS-Scar females were crossed to twi-GAL4, scar$^{\Delta 37}$/CyO,arm-GFP, sns-GAL4, scar$^{\Delta 37}$/CyO, ftz-lacZ or rP298-GAL4/Y;scar$^{\Delta 37}$/CyO, ftz-lacZ males. Scar rescue of *sltr–sltr* ^{S1946}*/CyO, arm-GFP; UAS-Scar* females were crossed with *twi-GAL4, sltr* ^{S1946}*/CyO, actin-lacZ* males. The *scar* or *sltr* homozygous mutant embryos were identified by the lack of anti–β-gal and anti-GFP staining. Transgene expression was confirmed with anti-Scar antibody staining. Two independent transgenes were tested for each rescue experiment.

Molecular biology

Characterization of the *scar*^{S196} allele. The molecular lesion of *scar*^{S196} was determined by sequencing the genomic DNA PCR amplified from homozygous mutant embryos identified by the absence of GFP expression from the mutant stock *w; scar*^{S196}*/CyO,arm-GFP*. Sequencing analysis revealed a single nucleotide insertion (T) in the fourth exon that caused a frameshift mutation leading to premature termination at amino acid 436.

Making Scar rescue constructs. Full-length *scar* was amplified by PCR (with or without a V5 tag) from EST clone SD02991 obtained from the Drosophila Genomics Resource Center (DGRC; Bloomington, IN). These PCR fragments were then subcloned into the transformation vector pUAST and both constructs were verified by sequencing analysis.

Making UAS-mCherry-CAAX. The mCherry coding sequence was amplified from pmCherry (a kind gift of R.Y. Tsien, University of California, San Diego, La Jolla, CA), and cloned into the EcoRI and XhoI sites of pUAST vector with the following primer set: forward: 5′-GGGGAATTCCAACATGGTGAGCAAGGGCGAGG-3′, reverse: 5′-GGGCTCGAGCTACATCAGGCAGCACTTCCTCTTGCCCTTCTTCTTGTAATCCTGCTTGTACAGCTCGTCCATGCC-3′. The reverse primer contains 14 amino acids of the CAAX membrane-targeting motif of *Drosophila* Ras2 (modified from Kakihara et al., 2008).

Immunohistochemistry

Embryos were fixed and stained as described previously (Kim et al., 2007). Primary and secondary antibodies were added and incubated overnight at 4°C. For phalloidin staining, embryos were fixed in formaldehyde-saturated heptane (1:1 mix of 37% formaldehyde and heptane, shaken well and left overnight) for 1 h at room temperature, then hand-devitellinized in PBST. FITC-conjugated phalloidin was added with both primary and secondary antibodies. Phalloidin–Fluorescein isothiocyanate (Sigma-Aldrich) was diluted to 20 µM in methanol and used (1:250) to mark F-actin. The following antibodies were used: rabbit anti-MHC (1:1,000; Kiehart and Feghali, 1986); rabbit anti-GFP (1:1,000; Invitrogen); mouse anti-GFP (1:500; Invitrogen); rabbit anti–β-gal (1:1,000; Cappel); mouse anti–β-gal (1:1,000; Promega); mouse anti-mCherry (1:250; Takara Bio Inc.); rabbit anti-Sns (1:400; Galletta et al., 2004); rabbit anti-Lmd (1:500; Duan et al., 2001); mouse anti-Eve (1:30; Developmental Studies Hybridoma Bank, Iowa City, IA); rat anti-Sltr (1:50; Kim et al., 2007); guinea pig anti-Scar (1:100 or 150; Zallen et al., 2002). A polyclonal guinea pig anti-Ants antiserum was generated using a C-terminal peptide (BioSynthesis) and used at 1:1,000. Guinea pig anti-Duf antiserum was generated against an N-terminal peptide (BioSynthesis), purified with a Sulfolink kit according to the manufacturer's instructions (Thermo Fisher Scientific), and used at 1:250. Secondary antibodies used at 1:300 were: FITC-, Cy3-, and Cy5-conjugated (Jackson ImmunoResearch Laboratories, Inc.) and biotinylated (Vector Laboratories) antibodies made in goat. Vectastain ABC kit (Vector Laboratories) and the TSA system (PerkinElmer) were used to amplify Sltr, Eve, β-gal, and Scar fluorescent signals.

Confocal imaging of fixed samples

Images were obtained on a confocal microscope (LSM 510; Carl Zeiss, Inc.) with Fluar 40x, 1.3 NA oil and Plan-Apochromat 100x 1.4 NA oil DIC objectives (Carl Zeiss, Inc.), Argon 458-, 477-, 488-, 514-nm; HeNe 543-nm; and HeNe 633-nm lasers, and the META detector. The pinhole was set to 1.0 AU for each channel and images were collected at 1.0-µm intervals for 40x and 0.5-µm intervals for 100x. Images were acquired with LSM Image Browser software (Carl Zeiss, Inc.) and processed using Adobe Photoshop CS. All samples were mounted in Vectashield (Vector Laboratories) and imaged at room temperature.

For three-dimensional reconstruction, Z stacks were collected at 0.3-µm intervals and reconstructions were generated using Volocity software (Improvision) and animated with QuickTime (Apple).

Time-lapse imaging

Before embryo collection, a thin layer of heptane glue was applied onto a clean microscope glass slide and let dry. Embryos were collected, dechorionated with bleach, thoroughly washed, and gently attached onto the dried heptane glue, which keeps embryos from rolling and drifting. Subsequently, embryos were covered with a few drops of distilled water to keep them moist while allowing adequate oxygen exchange. Fluorescent GFP-actin was visualized with a Plan-Apochromat 63x, 1.0 NA Vis-IR or 40x 0.8 NA IR Achroplan water objective (Carl Zeiss, Inc.). The Argon laser output was set to 10% to avoid photobleaching and phototoxicity. Other confocal settings are as follows: pixel time 0.8 µs; 8 frames were averaged per scan; z-stack 8-µm total, 1 µm step-wise; pinhole was generally set to 0.67 AU. LSM Image Browser 4.2 (Carl Zeiss, Inc.) and ImageJ 1.41h (Wayne Rasband, National Institutes of Health, Bethesda, MD) were used to convert confocal images to movies.

Transmission electron microscopy

HPF/FS fixation was performed as described previously (Zhang and Chen, 2008). In brief, a Bal-Tec device was used to freeze embryos. Freeze-substitution was performed using 1% osmium tetroxide and 0.1% uranyl acetate in 98% acetone and 2% methanol on dry ice. The embryos were embedded in EPON (Sigma-Aldrich), and sectioned and stained with 5% uranyl acetate for 10 min. Lead staining was done according to Sato (1968), and images were acquired on a transmission electron microscope (model CM120; Philips).

Conventional chemical fixation was performed at room temperature as described previously (Zhang and Chen, 2008). In brief, embryos were fixed in heptane equilibrated with 25% glutaraldehyde/10% acrolein in 0.1 M sodium cacodylate buffer, pH 7.4. Postfixation was performed with osmium tetroxide and embryos were stained with 1% uranyl acetate before embedding in EPON (Sigma-Aldrich). Embryos were then sectioned and stained with 5% uranyl acetate for 10 min. Lead staining was done according to Sato (1968) and images were acquired on a transmission electron microscope (model CM120; Philips).

Post-acquisition measurements

F-actin foci size was measured by tracing the outline of the actin focus, using the intensity information as a guide of foci boundaries. To be included as part of the foci, the intensity of phalloidin signal in the pixel had to be greater than the average intensity of the cortical actin. The area was calculated using the Zeiss LSM software. Foci were measured if they could be assigned to one FCM and were distinct from other foci, to ensure that only a single focus was measured.

Online supplemental material

Fig. S1 shows colocalization of cell type–specific markers and F-actin foci at sites of fusion. Fig. S2 shows leaky expression of the founder cell–"specific" *rP298-GAL4* driver in a small number of FCMs. Fig. S3 shows electron micrographs of serial sections of three invasive F-actin foci. Fig. S4 shows that myoblast fusion is severely blocked in *scar sltr* double mutants and the requirement of Scar in both muscle cell types. Fig. S5 shows lack of GFP diffusion in *dWIP* and *kette* mutant embryos. Video 1 shows live imaging of a fusion event between a single FCM and a multinucleated myotube. Videos 2–4 show live imaging of actin foci in embryos expressing GFP-actin with pan-mesodermal or cell type–specific drivers. Video 5 shows 3D reconstruction of invasive FCM-specific F-actin foci and the corresponding cup-shaped dimple on founder cell membrane. Table S1 shows mean number of nuclei in the DA1 muscle in wild-type and single- or double-fusion mutants. Table S2 shows mean number of nuclei in DA1 muscle in rescued fusion mutants. Online supplemental material is available at http://www.jcb.org/cgi/content/full/jcb.201006006/DC1.

We thank Drs. S. Abmayr, D. Andrew, D. Kiehart, D. Menon, M. Ruiz-Gómez, E. Schejter, J. Zallen, and A. Zelhof for antibodies and fly stocks; Dr. Richard Leapman at LBPH, National Institutes of Health, for access to the HPF/FS unit; Nathan Anderson and Taylor Mann for technical assistance; and Drs. Debbie Andrew, Sue Craig, Chen-Ming Fan, Eric Grote, D.J. Pan, Doug Robinson, Geraldine Seydoux, and members of the Chen laboratory for helpful discussions and comments on the manuscript.

This work was supported by grants from the National Institutes of Health and the American Heart Association. P. Jin is a predoctoral fellow of the American Heart Association. E.H. Chen is a Searle Scholar and a Packard Fellow.

Submitted: 1 June 2010
Accepted: 26 October 2010

References

Abmayr, S.M., S. Zhuang, and E.R. Geisbrecht. 2008. Myoblast fusion in *Drosophila*. *Methods Mol. Biol.* 475:75–97. doi:10.1007/978-1-59745-250-2_5

Albiges-Rizo, C., O. Destaing, B. Fourcade, E. Planus, and M.R. Block. 2009. Actin machinery and mechanosensitivity in invadopodia, podosomes and focal adhesions. *J. Cell Sci.* 122:3037–3049. doi:10.1242/jcs.052704

Artero, R.D., I. Castanon, and M.K. Baylies. 2001. The immunoglobulin-like protein Hibris functions as a dose-dependent regulator of myoblast fusion and is differentially controlled by Ras and Notch signaling. *Development.* 128:4251–4264.

Baylies, M.K., M. Bate, and M. Ruiz Gomez. 1998. Myogenesis: a view from *Drosophila*. *Cell.* 93:921–927. doi:10.1016/S0092-8674(00)81198-8

Beckett, K., and M.K. Baylies. 2007. 3D analysis of founder cell and fusion competent myoblast arrangements outlines a new model of myoblast fusion. *Dev. Biol.* 309:113–125. doi:10.1016/j.ydbio.2007.06.024

Ben-Yaacov, S., R. Le Borgne, I. Abramson, F. Schweisguth, and E.D. Schejter. 2001. Wasp, the *Drosophila* Wiskott-Aldrich syndrome gene homologue, is required for cell fate decisions mediated by Notch signaling. *J. Cell Biol.* 152:1–13.

Berger, S., G. Schäfer, D.A. Kesper, A. Holz, T. Eriksson, R.H. Palmer, L. Beck, C. Klämbt, R. Renkawitz-Pohl, and S.F. Onel. 2008. WASP and SCAR have distinct roles in activating the Arp2/3 complex during myoblast fusion. *J. Cell Sci.* 121:1303–1313. doi:10.1242/jcs.022269

Billadeau, D.D., J.C. Nolz, and T.S. Gomez. 2007. Regulation of T-cell activation by the cytoskeleton. *Nat. Rev. Immunol.* 7:131–143. doi:10.1038/nri2021

Bour, B.A., M. Chakravarti, J.M. West, and S.M. Abmayr. 2000. *Drosophila* SNS, a member of the immunoglobulin superfamily that is essential for myoblast fusion. *Genes Dev.* 14:1498–1511.

Brugnera, E., L. Haney, C. Grimsley, M. Lu, S.F. Walk, A.C. Tosello-Trampont, I.G. Macara, H. Madhani, G.R. Fink, and K.S. Ravichandran. 2002. Unconventional Rac-GEF activity is mediated through the Dock180-ELMO complex. *Nat. Cell Biol.* 4:574–582.

Carman, C.V. 2009. Mechanisms for transcellular diapedesis: probing and path-finding by 'invadosome-like protrusions'. *J. Cell Sci.* 122:3025–3035. doi:10.1242/jcs.047522

Carman, C.V., P.T. Sage, T.E. Sciuto, M.A. de la Fuente, R.S. Geha, H.D. Ochs, H.F. Dvorak, A.M. Dvorak, and T.A. Springer. 2007. Transcellular diapedesis is initiated by invasive podosomes. *Immunity.* 26:784–797. doi:10.1016/j.immuni.2007.04.015

Chen, E.H., and E.N. Olson. 2001. Antisocial, an intracellular adaptor protein, is required for myoblast fusion in *Drosophila*. *Dev. Cell.* 1:705–715. doi:10.1016/S1534-5807(01)00084-3

Chen, E.H., and E.N. Olson. 2005. Unveiling the mechanisms of cell-cell fusion. *Science.* 308:369–373. doi:10.1126/science.1104799

Chen, E.H., B.A. Pryce, J.A. Tzeng, G.A. Gonzalez, and E.N. Olson. 2003. Control of myoblast fusion by a guanine nucleotide exchange factor, loner, and its effector ARF6. *Cell.* 114:751–762. doi:10.1016/S0092-8674(03)00720-7

Chen, E.H., E. Grote, W. Mohler, and A. Vignery. 2007. Cell-cell fusion. *FEBS Lett.* 581:2181–2193. doi:10.1016/j.febslet.2007.03.033

Chen, A., E. Leikina, K. Melikov, B. Podbilewicz, M.M. Kozlov, and L.V. Chernomordik. 2008. Fusion-pore expansion during syncytium formation is restricted by an actin network. *J. Cell Sci.* 121:3619–3628. doi:10.1242/jcs.032169

Dillon, C., and Y. Goda. 2005. The actin cytoskeleton: integrating form and function at the synapse. *Annu. Rev. Neurosci.* 28:25–55. doi:10.1146/annurev.neuro.28.061604.135757

Doberstein, S.K., R.D. Fetter, A.Y. Mehta, and C.S. Goodman. 1997. Genetic analysis of myoblast fusion: blown fuse is required for progression beyond the prefusion complex. *J. Cell Biol.* 136:1249–1261. doi:10.1083/jcb.136.6.1249

Duan, H., J.B. Skeath, and H.T. Nguyen. 2001. *Drosophila* Lame duck, a novel member of the Gli superfamily, acts as a key regulator of myogenesis by controlling fusion-competent myoblast development. *Development.* 128:4489–4500.

Dustin, M.L., and D.R. Colman. 2002. Neural and immunological synaptic relations. *Science.* 298:785–789. doi:10.1126/science.1076386

Dvoráková, K., H.D. Moore, N. Sebková, and J. Palecek. 2005. Cytoskeleton localization in the sperm head prior to fertilization. *Reproduction.* 130:61–69. doi:10.1530/rep.1.00549

Dworak, H.A., M.A. Charles, L.B. Pellerano, and H. Sink. 2001. Characterization of *Drosophila hibris*, a gene related to human nephrin. *Development.* 128:4265–4276.

Erickson, M.R., B.J. Galletta, and S.M. Abmayr. 1997. *Drosophila myoblast city* encodes a conserved protein that is essential for myoblast fusion, dorsal closure, and cytoskeletal organization. *J. Cell Biol.* 138:589–603. doi:10.1083/jcb.138.3.589

Galletta, B.J., M. Chakravarti, R. Banerjee, and S.M. Abmayr. 2004. SNS: Adhesive properties, localization requirements and ectodomain dependence in S2 cells and embryonic myoblasts. *Mech. Dev.* 121:1455–1468. doi:10.1016/j.mod.2004.08.001

Gammie, A.E., V. Brizzio, and M.D. Rose. 1998. Distinct morphological phenotypes of cell fusion mutants. *Mol. Biol. Cell.* 9:1395–1410.

Gildor, B., R. Massarwa, B.Z. Shilo, and E.D. Schejter. 2009. The SCAR and WASp nucleation-promoting factors act sequentially to mediate *Drosophila* myoblast fusion. *EMBO Rep.* 10:1043–1050. doi:10.1038/embor.2009.129

Gimona, M., R. Buccione, S.A. Courtneidge, and S. Linder. 2008. Assembly and biological role of podosomes and invadopodia. *Curr. Opin. Cell Biol.* 20:235–241. doi:10.1016/j.ceb.2008.01.005

Hummel, T., K. Leifker, and C. Klämbt. 2000. The *Drosophila* HEM-2/NAP1 homolog KETTE controls axonal pathfinding and cytoskeletal organization. *Genes Dev.* 14:863–873.

Jay, S.M., E. Skokos, F. Laiwalla, M.M. Krady, and T.R. Kyriakides. 2007. Foreign body giant cell formation is preceded by lamellipodia formation and can be attenuated by inhibition of Rac1 activation. *Am. J. Pathol.* 171:632–640. doi:10.2353/ajpath.2007.061213

Kakihara, K., K. Shinmyozu, K. Kato, H. Wada, and S. Hayashi. 2008. Conversion of plasma membrane topology during epithelial tube connection requires Arf-like 3 small GTPase in *Drosophila*. *Mech. Dev.* 125:325–336. doi:10.1016/j.mod.2007.10.012

Kaplan, D., J. Zimmerberg, A. Puri, D.P. Sarkar, and R. Blumenthal. 1991. Single cell fusion events induced by influenza hemagglutinin: studies with rapid-flow, quantitative fluorescence microscopy. *Exp. Cell Res.* 195:137–144. doi:10.1016/0014-4827(91)90509-S

Kesper, D.A., C. Stute, D. Buttgereit, N. Kreisköther, S. Vishnu, K.F. Fischbach, and R. Renkawitz-Pohl. 2007. Myoblast fusion in *Drosophila melanogaster* is mediated through a fusion-restricted myogenic-adhesive structure (FuRMAS). *Dev. Dyn.* 236:404–415. doi:10.1002/dvdy.21035

Kiehart, D.P., and R. Feghali. 1986. Cytoplasmic myosin from *Drosophila melanogaster*. *J. Cell Biol.* 103:1517–1525. doi:10.1083/jcb.103.4.1517

Kim, S., K. Shilagardi, S. Zhang, S.N. Hong, K.L. Sens, J. Bo, G.A. Gonzalez, and E.H. Chen. 2007. A critical function for the actin cytoskeleton in targeted exocytosis of prefusion vesicles during myoblast fusion. *Dev. Cell.* 12:571–586. doi:10.1016/j.devcel.2007.02.019

Kocherlakota, K.S., J.M. Wu, J. McDermott, and S.M. Abmayr. 2008. Analysis of the cell adhesion molecule sticks-and-stones reveals multiple redundant functional domains, protein-interaction motifs and phosphorylated tyrosines that direct myoblast fusion in *Drosophila melanogaster*. *Genetics.* 178:1371–1383. doi:10.1534/genetics.107.083808

Kurisu, S., and T. Takenawa. 2009. The WASP and WAVE family proteins. *Genome Biol.* 10:226. doi:10.1186/gb-2009-10-6-226

Linder, S. 2007. The matrix corroded: podosomes and invadopodia in extracellular matrix degradation. *Trends Cell Biol.* 17:107–117. doi:10.1016/j.tcb.2007.01.002

Linder, S. 2009. Invadosomes at a glance. *J. Cell Sci.* 122:3009–3013. doi:10.1242/jcs.032631

Massarwa, R., S. Carmon, B.Z. Shilo, and E.D. Schejter. 2007. WIP/WASp-based actin-polymerization machinery is essential for myoblast fusion in *Drosophila*. *Dev. Cell.* 12:557–569. doi:10.1016/j.devcel.2007.01.016

Mattila, P.K., and P. Lappalainen. 2008. Filopodia: molecular architecture and cellular functions. *Nat. Rev. Mol. Cell Biol.* 9:446–454. doi:10.1038/nrm2406

McDonald, K.L., and M. Auer. 2006. High-pressure freezing, cellular tomography, and structural cell biology. *Biotechniques.* 41:137: 139: 141 passim. doi:10.2144/000112226

Menon, S.D., and W. Chia. 2001. *Drosophila rolling pebbles*: a multidomain protein required for myoblast fusion that recruits D-Titin in response to the myoblast attractant Dumbfounded. *Dev. Cell.* 1:691–703. doi:10.1016/S1534-5807(01)00075-2

Mohler, W.A., J.S. Simske, E.M. Williams-Masson, J.D. Hardin, and J.G. White. 1998. Dynamics and ultrastructure of developmental cell fusions in the *Caenorhabditis elegans* hypodermis. *Curr. Biol.* 8:1087–1090. doi:10.1016/S0960-9822(98)70447-6

Oren-Suissa, M., and B. Podbilewicz. 2007. Cell fusion during development. *Trends Cell Biol.* 17:537–546.

Pajcini, K.V., J.H. Pomerantz, O. Alkan, R. Doyonnas, and H.M. Blau. 2008. Myoblasts and macrophages share molecular components that contribute to cell-cell fusion. *J. Cell Biol.* 180:1005–1019. doi:10.1083/jcb.200707191

Plonsky, I., and J. Zimmerberg. 1996. The initial fusion pore induced by baculovirus GP64 is large and forms quickly. *J. Cell Biol.* 135:1831–1839. doi:10.1083/jcb.135.6.1831

Plonsky, I., M.S. Cho, A.G. Oomens, G. Blissard, and J. Zimmerberg. 1999. An analysis of the role of the target membrane on the Gp64-induced fusion pore. *Virology.* 253:65–76. doi:10.1006/viro.1998.9493

Prokop, A., M.D. Martín-Bermudo, M. Bate, and N.H. Brown. 1998. Absence of PS integrins or laminin A affects extracellular adhesion, but not intracellular assembly, of hemiadherens and neuromuscular junctions in *Drosophila* embryos. *Dev. Biol.* 196:58–76. doi:10.1006/dbio.1997.8830

Quintavalle, M., L. Elia, G. Condorelli, and S.A. Courtneidge. 2010. MicroRNA control of podosome formation in vascular smooth muscle cells in vivo and in vitro. *J. Cell Biol.* 189:13–22. doi:10.1083/jcb.200912096

Rau, A., D. Buttgereit, A. Holz, R. Fetter, S.K. Doberstein, A. Paululat, N. Staudt, J. Skeath, A.M. Michelson, and R. Renkawitz-Pohl. 2001. *rolling pebbles* (rols) is required in *Drosophila* muscle precursors for recruitment of myoblasts for fusion. *Development.* 128:5061–5073.

Richardson, B.E., K. Beckett, S.J. Nowak, and M.K. Baylies. 2007. SCAR/WAVE and Arp2/3 are crucial for cytoskeletal remodeling at the site of myoblast fusion. *Development.* 134:4357–4367. doi:10.1242/dev.010678

Rochlin, K., S. Yu, S. Roy, and M.K. Baylies. 2010. Myoblast fusion: when it takes more to make one. *Dev. Biol.* 341:66–83. doi:10.1016/j.ydbio.2009.10.024

Rottiers, P., F. Saltel, T. Daubon, B. Chaigne-Delalande, V. Tridon, C. Billottet, E. Reuzeau, and E. Génot. 2009. TGFbeta-induced endothelial podosomes mediate basement membrane collagen degradation in arterial vessels. *J. Cell Sci.* 122:4311–4318. doi:10.1242/jcs.057448

Ruiz-Gómez, M., N. Coutts, A. Price, M.V. Taylor, and M. Bate. 2000. *Drosophila* dumbfounded: a myoblast attractant essential for fusion. *Cell.* 102:189–198. doi:10.1016/S0092-8674(00)00024-6

Salinas, P.C., and S.R. Price. 2005. Cadherins and catenins in synapse development. *Curr. Opin. Neurobiol.* 15:73–80. doi:10.1016/j.conb.2005.01.001

Sato, T. 1968. A modified method for lead staining of thin sections. *J. Electron Microsc. (Tokyo).* 17:158–159.

Schäfer, G., S. Weber, A. Holz, S. Bogdan, S. Schumacher, A. Müller, R. Renkawitz-Pohl, and S.F. Onel. 2007. The Wiskott-Aldrich syndrome protein (WASP) is essential for myoblast fusion in *Drosophila*. *Dev. Biol.* 304:664–674. doi:10.1016/j.ydbio.2007.01.015

Shelton, C., K.S. Kocherlakota, S. Zhuang, and S.M. Abmayr. 2009. The immunoglobulin superfamily member Hbs functions redundantly with Sns in interactions between founder and fusion-competent myoblasts. *Development.* 136:1159–1168. doi:10.1242/dev.026302

Small, J.V., T. Stradal, E. Vignal, and K. Rottner. 2002. The lamellipodium: where motility begins. *Trends Cell Biol.* 12:112–120. doi:10.1016/S0962-8924(01)02237-1

Stinchcombe, J.C., and G.M. Griffiths. 2007. Secretory mechanisms in cell-mediated cytotoxicity. *Annu. Rev. Cell Dev. Biol.* 23:495–517. doi:10.1146/annurev.cellbio.23.090506.123521

Stradal, T.E., and G. Scita. 2006. Protein complexes regulating Arp2/3-mediated actin assembly. *Curr. Opin. Cell Biol.* 18:4–10. doi:10.1016/j.ceb.2005.12.003

Strünkelnberg, M., B. Bonengel, L.M. Moda, A. Hertenstein, H.G. de Couet, R.G. Ramos, and K.F. Fischbach. 2001. *rst* and its paralogue *kirre* act redundantly during embryonic muscle development in *Drosophila*. *Development.* 128:4229–4239.

Takenawa, T., and S. Suetsugu. 2007. The WASP-WAVE protein network: connecting the membrane to the cytoskeleton. *Nat. Rev. Mol. Cell Biol.* 8:37–48. doi:10.1038/nrm2069

Tilney, L.G., and D.A. Portnoy. 1989. Actin filaments and the growth, movement, and spread of the intracellular bacterial parasite, Listeria monocytogenes. *J. Cell Biol.* 109:1597–1608. doi:10.1083/jcb.109.4.1597

Zallen, J.A., Y. Cohen, A.M. Hudson, L. Cooley, E. Wieschaus, and E.D. Schejter. 2002. SCAR is a primary regulator of Arp2/3-dependent morphological events in *Drosophila*. *J. Cell Biol.* 156:689–701. doi:10.1083/jcb.200109057

Zhang, S., and E.H. Chen. 2008. Ultrastructural analysis of myoblast fusion in *Drosophila*. *In* Cell Fusion: Overviews and Methods. E.H. Chen, editor. Humana Press, NJ. 275–297.